

Impurity Moments Conceal Low-Energy Relaxation of Quantum Spin Liquids

A. Pustogow,¹ T. Le,¹ H.-H. Wang,¹ Yongkang Luo,¹ E. Gati,² H. Schubert,² M. Lang,² and S. E. Brown¹

¹*Department of Physics and Astronomy, UCLA, Los Angeles, California 90095, USA*

²*Institute of Physics, Goethe-University Frankfurt, 60438 Frankfurt (Main), Germany*

(Dated: November 7, 2019)

We scrutinize the magnetic properties of κ -(BEDT-TTF)₂Hg(SCN)₂Cl through its first-order metal-insulator transition at $T_{\text{CO}} = 30$ K by means of ¹H nuclear magnetic resonance (NMR). While in the metal we find Fermi-liquid behavior with temperature-independent $(T_1T)^{-1}$, the relaxation rate exhibits a pronounced enhancement when charge order sets in. The NMR spectra remain unchanged through the transition and no magnetic order stabilizes down to 25 mK. Similar to the isostructural spin-liquid candidates κ -(BEDT-TTF)₂Cu₂(CN)₃ and κ -(BEDT-TTF)₂Ag₂(CN)₃, T_1^{-1} acquires a dominant maximum (here around 5 K). Field-dependent experiments identify the low-temperature feature as a dynamic inhomogeneity contribution that is typically dominant over the intrinsic relaxation but gets suppressed with magnetic field.

The rise and fall of antiferromagnetism (AFM) in correlated electron systems is intensely debated in the context of quantum spin liquids (QSL) [1–3]. These elusive states of matter are expected to host exotic quasiparticles, such as neutral spinons or Majorana fermions, and have been advanced as possible platforms for quantum information applications. Following the original work of Anderson [4], Mott insulators on frustrated lattices are considered a natural starting point for QSL realization. In this context, insulating charge-transfer salts were among the first QSL candidate systems: the compounds κ -(BEDT-TTF)₂Cu₂(CN)₃ (abbreviated κ -CuCN), κ -(BEDT-TTF)₂Ag₂(CN)₃ (κ -AgCN) and β' -EtMe₃Sb[Pd(dmit)₂]₂ (β' -EtMe) are well described by anisotropic triangular-lattice models [5, 6], and are observed to avoid long-range order to the lowest temperatures measured [7, 8]. Consequently, the nature of the ground state, as well as the factors influencing the suppression of magnetic order have been of central importance. With respect to the former, the presence of gapless fermionic excitations has been inferred from thermodynamic probes including specific heat and spin susceptibility [9–11], as well as NMR spin-lattice relaxation [7, 8, 12]. In some cases, thermal transport and electrodynamic measurements [13–15] have provided evidence that these gapless excitations are also mobile [16].

The so-called κ -phase molecular solids provide a versatile playground to study the interplay of spin and charge for varying degree of electronic correlations and geometrical frustration. In the prototypical Mott insulators κ -CuCN and κ -(BEDT-TTF)₂Cu[N(CN)₂]Cl (κ -CuCl), pairs of BEDT-TTF molecules are strongly coupled ($t_d \gg t, t'$, cf. Fig. 1a,b), establishing a textbook-type realization of the single-band Hubbard model at 1/2 filling [5], even on quantitative scales [17]. Despite comparable exchange interaction $J/k_B \approx 200$ K, the latter compound has an AFM ground state [18] while the former exhibits no magnetic order and is therefore considered as a promising QSL candidate [7, 19]. Highlighting the role of frustration [1, 20] in determining these dis-

parate outcomes, despite similar structural and electronic properties, is the proposal that AFM in κ -CuCl is linked to the charge degrees of freedom [21]. That is, the detection of a dielectric anomaly [21] and pronounced phonon renormalization effects [22] close to the AFM transition were assigned to intra-dimer charge degrees of freedom. It was suggested [21] that charge order (CO) may reduce frustration giving rise to an ordered ground state. As well, quenched disorder [23], disorder [24–30], low dimensionality [1, 31], and proximity to the Mott transition [32] have all been cited as potentially key considerations.

A promising route to disentangle the underlying mechanisms is to introduce additional symmetry breaking. Compounds comprised of the Hg-based anions (Hg(SCN)₂X, X=Cl, Br) have recently come into focus [33–41] due to the tendency towards electronic CO. The weaker dimerization (the ratios t_d/t are closer to unity [42]) increase the relative importance of inter-site Coulomb repulsion. In κ -(BEDT-TTF)₂Hg(SCN)₂Cl (κ -HgCl) the metal-insulator transition (MIT) at $T_{\text{CO}} = 30$ K is very similar to CO in α -(BEDT-TTF)₂I₃, also exhibiting a discontinuous symmetry breaking [34, 35, 37, 43, 44]. While the charge sector of κ -HgCl [33–35, 41] has been investigated in great detail, no definitive conclusion was achieved on the spin degrees of freedom [33, 37]. Particularly in view of the closely related κ -(BEDT-TTF)₂Hg(SCN)₂Br (κ -HgBr), where recently an exotic dipole-liquid state [40] and indications for ferromagnetism [38] were reported, the magnetic ground state and possible spin-charge coupling call for clarification.

In this Letter we investigate the low-energy magnetic properties of κ -(BEDT-TTF)₂Hg(SCN)₂Cl via ¹H nuclear magnetic resonance (NMR). In the metallic phase we observe Fermi-liquid behavior with constant $(T_1T)^{-1}$ while for $25 \text{ mK} \leq T < T_{\text{CO}}$ spectroscopic measurements find no evidence for magnetic order. T_1^{-1} exhibits a dominant maximum around 5 K with pronounced magnetic field and temperature dependences characteristic of $S=1/2$, $g=2$ impurity states. Notably, the overall behavior is decidedly similar to that reported for the well-

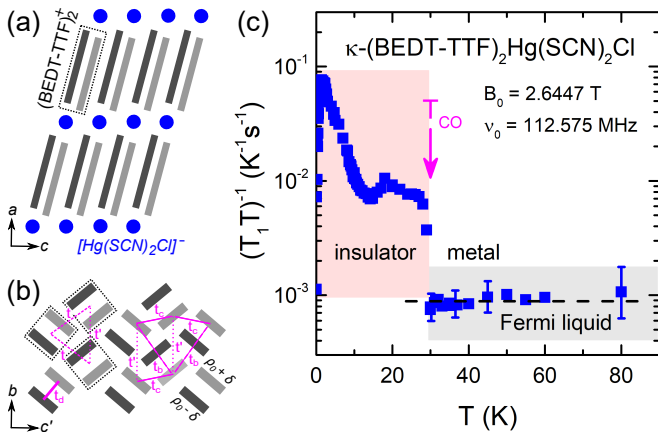


FIG. 1. (a) κ -(BEDT-TTF) $_2$ Hg(SCN) $_2$ Cl crystals consist of monovalent anions (blue) separating the conducting BEDT-TTF cation layers which acquire inequivalent site charges (dark and light grey) in the charge-ordered state. (b) Dimerized in-plane arrangement with a stripe pattern of charge-rich ($\rho_0 + \delta$; $\rho_0 = 0.5$ e) and -poor ($\rho_0 - \delta$) molecules [34, 37]. The magenta lines indicate transfer integrals t_i among (BEDT-TTF) $_2^+$ dimers (black dotted lines) and between charge-rich sites, respectively [37]. (c) In the metallic state $(T_1T)^{-1}$ is T -independent, in accord with Fermi-liquid behavior [33–35]. A pronounced jump appears at the first-order MIT at T_{CO} .

known κ -phase QSL candidates, κ -CuCN and κ -AgCN. As we will argue below, it appears that the dynamic low-temperature contribution is a common feature in all these compounds without magnetic order and originates from inhomogeneities rather than intrinsic spin degrees of freedom. We quantitatively link T_1^{-1} to impurity states detected by ESR [33, 37].

κ -(BEDT-TTF) $_2$ Hg(SCN) $_2$ Cl single crystals with typical dimensions of $1 \times 0.5 \times 0.3$ mm were grown by electrochemical methods reported elsewhere [37]. NMR experiments were performed with home-built spectrometers utilizing superconducting magnets. For sample 1, the field strength was $B_0 = 2.6447$ T, with alignment close to $\mathbf{B}_0 \parallel c$. Field-dependent measurements (sample 2; \mathbf{B}_0 out-of-plane) covered the range 1.2–9.3 T. Standard ^4He flow cryostats were employed above 1.6 K whereas a $^3\text{He}/^4\text{He}$ dilution refrigerator allowed us to access the range down to 25 mK. The spin-lattice relaxation rate was determined via free-induction decay following saturation, and analyzed using stretched-exponential fits.

The crystal structure of κ -HgCl consists of layers of positively charged BEDT-TTF molecules separated by monovalent anions, see Fig. 1(a,b). Within the conducting planes the organic cations are arranged in weakly bound pairs ($t_d/t' \approx 3$) assembled in an anisotropic triangular lattice ($t'/t = 0.79$ [37]), suggesting significant geometrical frustration. For $T < T_{CO}$, the electronic charge is redistributed between the two sites within a dimer, likely forming a stripe-like pattern [34, 37] that alters the magnetic frustration. Fig. 1(c) shows the variation

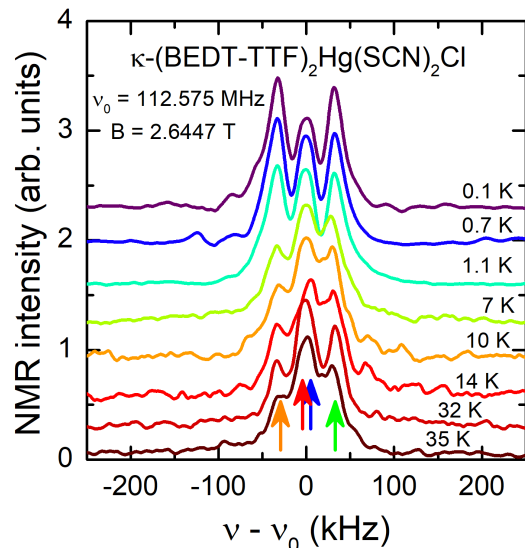


FIG. 2. The shape and width of the ^1H NMR spectra remains unaffected upon cooling through $T_{CO} = 30$ K, ruling out magnetic order down to mK temperatures. The NMR intensity was normalized with respect to the $1/T$ enhancement; curves were shifted vertically. The minor difference in relative amplitudes of inner and outer peaks below and above 2 K is due to slightly different sample alignment in different cryostats.

of $(T_1T)^{-1}$ with temperature, which is T -independent in the metallic state ($T > T_{CO}$). An abrupt jump appears at the transition signalling a change of the relevant energy scale from E_F in the metal (10^3 – 10^4 K) to J in the insulating state (10^2 K). The non-monotonic behavior upon further cooling will be discussed in the next paragraph. In Fig. 2 we show the ^1H NMR spectra for different temperatures, which appear to consist of four distinct peaks resulting from proton-proton dipolar coupling [45]. No significant modification of the peak structure is observed upon cooling below T_{CO} – clearly different to AFM in κ -CuCl [18]. Thus, the NMR spectra of κ -HgCl show no indications of magnetic order throughout the CO phase.

The spin-lattice relaxation rate T_1^{-1} is displayed on double-logarithmic scales in Fig. 3(a), covering the temperature range 0.025–80 K. For $T > T_{CO}$, the relaxation process proceeds homogeneously, as evident from the single-exponential recovery ($\alpha = 1$ in the stretched-exponential fit). Upon lowering T within the insulating state, T_1^{-1} first decreases, but then increases and peaks at $T \simeq 5$ K. In this range also stretched-exponential behavior sets in (initially $\alpha \approx 0.9$, see Fig. 3(a) inset). Well below the maximum T_1^{-1} exhibits a smooth, power-law like ($\propto T^2$) decrease on cooling further to $T \sim 25$ mK, in accord with the absence of AFM concluded from the NMR spectra (Fig. 2). Stretched-exponential behavior becomes more pronounced at the lowest measured temperatures – generally an indicator for a range of char-

acteristic relaxation time scales. In particular, $\alpha \approx 0.6$ results from a T_1^{-1} distribution spanning approximately one order of magnitude [46], which we illustrate by the red-white false-color plot behind the data in Fig. 3(a).

The low-temperature relaxation of κ -HgCl is reminiscent of the widely studied QSL candidates κ -CuCN, κ -AgCN and β' -EtMe. In those cases, power-law variation with temperature has been attributed to a gapless continuum of spin excitations [7, 12, 19, 47]. Here, we consider an alternative scenario: the proton T_1^{-1} at low temperatures is caused by dipolar coupling to localized $S = 1/2$, $g = 2$ spin degrees of freedom. The general idea is that the impurity spins, embedded in an otherwise nonmagnetic background, are sufficiently polarized in nonzero magnetic fields at low enough temperature, so as to progressively freeze out this relaxation channel, so as to progressively freeze out this relaxation channel. We note that low-temperature effects from disorder-induced spin defects were recently considered in Ref. [30].

The nuclear relaxation by dipolar coupling to magnetic impurities implies certain behaviors that can be compared to experiment. For example, T_1^{-1} of κ -AgCN is strongly reduced with increasing B_0 [12]; similar behavior is seen for κ -HgCl in Fig. 3(c). Here the field dependence is pronounced near the maxima around 5 K, while the relaxation for $T \simeq 10$ K remains rather unaffected. At a semi-quantitative level, this is precisely the temperature range corresponding to the Zeeman energy of a free spin. More specifically, the peak and low-temperature suppression of T_1^{-1} is modelled for a *single* proton as

$$T_1^{-1} = \frac{2}{5} \mu_o^2 \gamma_s^2 \gamma_I^2 \hbar^2 (S(S+1)) r^{-6} \frac{\tau}{1 + \omega^2 \tau^2}, \quad (1)$$

where $1/\tau$ is the bandwidth of longitudinal field fluctuations; it is taken to be of the form $\tau = \tau_0 e^{E_Z/k_B T}$, with $E_Z = g\mu_B S B_0$ the Zeeman energy splitting of the impurity spin levels, using $g = 2$ and $S = 1/2$. The activated behavior arises from the polarization of the impurity spins in the applied magnetic field. The dipolar coupling depends on the distance r between the impurity spin and the nuclear site. Naturally, random arrangement of the former is related to a distribution of local fields which results in a stretched-exponential recovery.

Looking at the Arrhenius plot in Fig. 3(b), the behavior on the low-temperature side of the maximum closely follows the associated thermal activation with $k_B T_0 \approx \mu_B B_0$ down to 0.2 K. The peak value in Fig. 3(c) roughly follows the expected $(T_1^{-1})_{max} \propto 1/B_0$ dependence, and $\tau = \omega^{-1}$ at the maximum yields τ_0 in the ns range, in agreement with the ESR linewidth $\Delta H \approx 3$ mT in the insulating state [37]. Plugging this into Eq. 1, together with our experimental values of T_1^{-1} , yields $r \approx 6-7$ nm. A similar result is obtained from the Curie behavior of the T -dependent ESR intensity [33, 37], giving an impurity concentration of order 10^{-2} per unit cell [34].

In Fig. 4(a) we compare T_1^{-1} of κ -HgCl with the isostructural QSL candidates κ -CuCN [7] and κ -AgCN

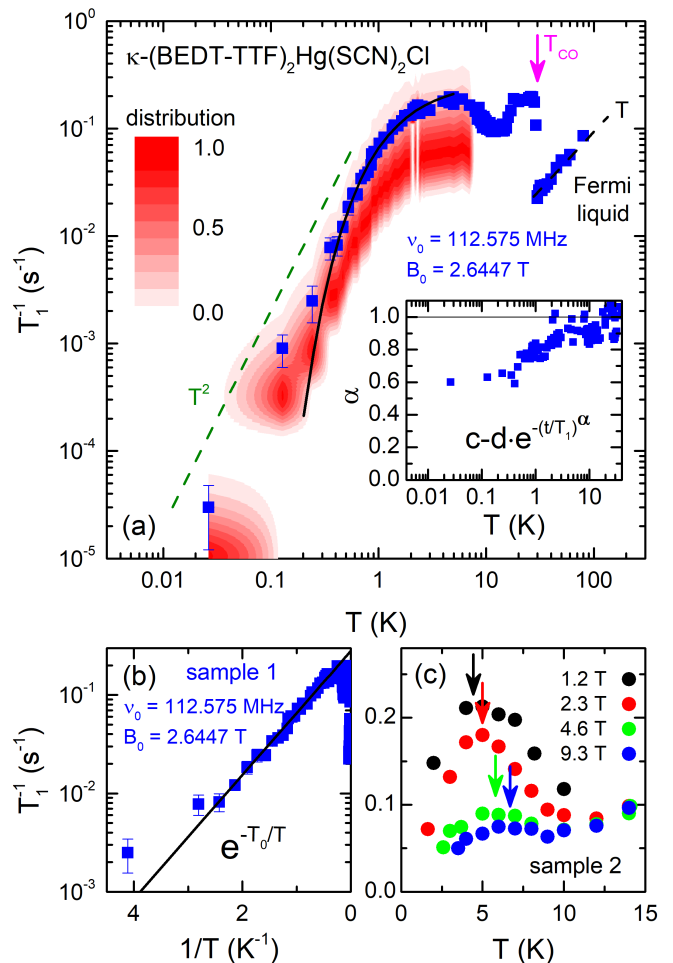


FIG. 3. (a) Subsequent to the abrupt increase at T_{CO} , the spin-lattice relaxation rate drops upon cooling, and a broad maximum forms around 5 K. Well below 1 K T_1^{-1} shows a power-law behavior similar to various spin-liquid candidates [7, 12, 19, 47]. Inset: The stretched-exponential recovery ($\alpha = 0.6$ at lowest T) reveals a continuum of low-energy decay channels; we visualize the related distribution of T_1^{-1} (according to Ref. 46) by the red-white false-color plot in the main graph. (b) Below the peak T_1^{-1} exhibits Arrhenius-like activation (black solid line; also indicated in (a)), with $k_B T_0 \approx \mu_B B_0$. (c) Upon increasing B_0 the maximum is strongly suppressed and shifts to higher T , in excellent agreement with Eq. 1 – even in the absolute values of T_1^{-1} .

[12] on common scales and for comparable B_0 as indicated. Although at different temperatures and not necessarily of the same origin, in all these compounds we identify a dynamic contribution with similar characteristics as elaborated above for κ -HgCl. Above the low-temperature maximum, $10 \text{ K} \leq T \leq 30 \text{ K}$, the data are similar in magnitude and follow an approximately linear temperature dependence; in the case of κ -CuCN and κ -AgCN, the behavior is attributed to gapless spinons. Generally, however, the quantitative similarity across compounds is not surprising in view of the comparable

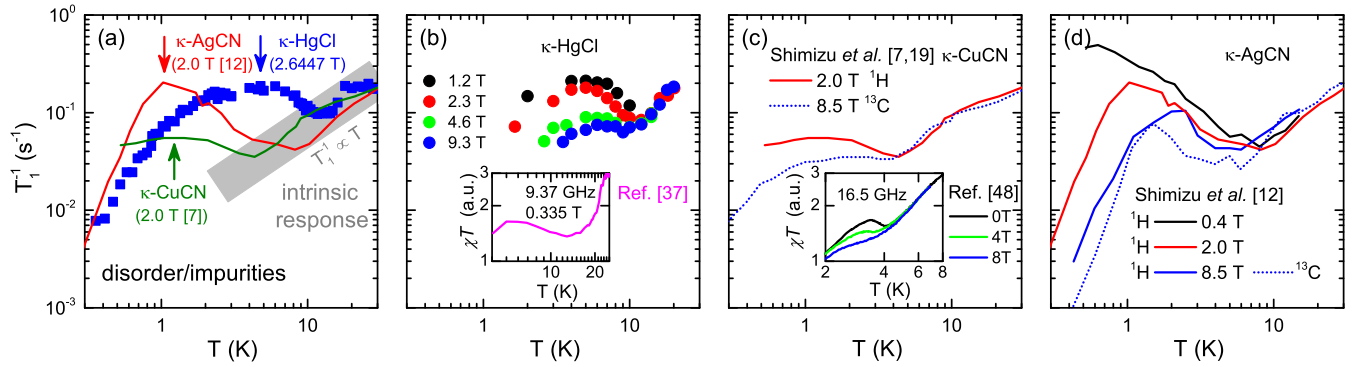


FIG. 4. (a) At temperatures above the maximum, the ^1H T_1^{-1} data in the insulating state of κ -HgCl coincide with the paradigmatic QSL candidates κ -CuCN and κ -AgCN. Here, T_1^{-1} follows a field-independent approximately linear T dependence suggesting that this is the intrinsic response with $J \approx 200$ K. (b-d) While peaked at different T_{max} , the low-temperature contribution exhibits a similar suppression with higher B_0 for all three compounds; ^{13}C data (scaled by γ_n [49]) match well with the ^1H results acquired at the same B_0 [7, 12, 19]. A similar field-dependent contribution is observed in high-frequency susceptibility data plotted as χT (inset of (b) at 9.37 GHz [37]; inset of (c) at 16.5 GHz [48]).

exchange energies. Since the dynamic maximum dominates a large range of the low-temperature relaxation, we cannot conclude whether there is a spin gap or not. High-field experiments ($k_B T_{max} < \mu_B B_0 < J$, i.e. a few tens of T) could possibly disclose the intrinsic magnetic properties of the QSL candidates down to low temperatures.

The overall suppression of the $g = 2$, $S = 1/2$ peak with increasing B_0 is similar for κ -HgCl and κ -AgCN, as summarized in Fig. 4(b,d). The published T_1^{-1} [12] on ^1H and ^{13}C [49] consistently show pronounced field dependence around the maximum, while the intrinsic response at higher T remains unaffected. A similar feature is also seen in the magnetic susceptibility: in the insets of (b,c) we show χT in order to compare to T_1^{-1} [37, 48]. Similar to κ -HgCl and κ -AgCN, the ^1H and ^{13}C data of κ -CuCN acquired at 2 and 8.5 T [7, 19], respectively, coincide above 4 K but deviate around the bump at lower T [Fig. 4(c)], where appreciable field dependence is also seen by different probes [48, 50, 51]. Due to the lack of consistent $T_1^{-1}(T)$ data upon varying B_0 , we do not exclude other contributions below 4 K in κ -CuCN.

Even though the NMR characteristics of κ -HgCl resemble the response of various QSL candidates in minute detail, its thermodynamic properties clearly indicate the absence of itinerant spin and charge excitations. That is, extrapolating C/T down to $T = 0$ yields a Sommerfeld coefficient non-distinguishable from zero [40], at least much smaller than for κ -CuCN and κ -AgCN where $\gamma \approx 10$ –20 mJK $^{-2}$ mol $^{-1}$ [9, 12]. Note, the sister compound κ -HgBr, where fluctuating CO has been suggested [40], exhibits γ comparable to the QSL candidates. Thus, the reduced entropy in κ -HgCl is consistent with gapped charge and spin degrees of freedom, for instance like in a valence bond solid. Similar to κ -CuCN [9], C/T from Ref. 40 reveals a Schottky-like increase to-

wards lower temperatures setting in at a few 100 mK, coincident with the power law in T_1^{-1} . It remains to elucidate to what extent disorder is relevant for the material under study – in particular in view of the stretched-exponential relaxation at low temperatures that suggests a continuum of low-energy decay channels.

The absolute values and temperature of the maximum in T_1^{-1} differ from compound to compound. If the origins were similar, this could be associated with a varying distribution of time scales τ . Performing a similar dipolar relaxation analysis for κ -CuCN and κ -AgCN yields slightly lower impurity densities than in κ -HgCl, but of similar order of magnitude (see Supplement). Finally, we comment briefly on the origin of the magnetic impurities in κ -HgCl. The clearly discontinuous phase transition at 30 K allows for the possibility of multiple CO domains and accompanying domain walls, as recently observed in $(\text{TMTTF})_2\text{X}$ by Raman spectroscopy [52]. A possible scenario is that the impurity states are located at domain walls. If that were the case, the absence of CO in κ -CuCN and κ -AgCN would point to a different origin of the dynamic contribution, likely linked to the anion layers [26, 27, 53]. Further, recent Raman experiments on κ -HgCl suggest BEDT-TTF $^{+0.5}$ below 10 K [41] which could also provide a source of $g = 2$, $S = 1/2$ spins.

To summarize, we map the low-energy spin dynamics in κ -(BEDT-TTF) $_2$ Hg(SCN) $_2$ Cl through the metal-insulator transition by comprehensive ^1H NMR experiments. The spin-lattice relaxation rate indicates a Fermi-liquid metal at elevated temperatures, and exhibits a pronounced discontinuous increase upon cooling through $T_{CO} = 30$ K into the charge-ordered phase. From the unaltered NMR spectra (Fig. 2) and the smooth temperature dependence of T_1^{-1} upon $T \rightarrow 0$ (Fig. 3), we conclude the absence of long-range magnetic order. Notably, we find that the magnetic response is essentially identi-

cal to isostructural QSL candidates [7, 12, 19], including the stretched-exponential recovery and a power-law like tail well below 1 K as well as a pronounced maximum in T_1^{-1} (peaked around 5 K in κ -HgCl). This low- T contribution exhibits a strong field dependence, very similar for κ -HgCl and κ -AgCN, likely originating from dipolar coupling to impurity spins. Taken together, these results imply that the low-temperature NMR properties in all these frustrated materials [7, 12, 19, 47] are dominated by extrinsic magnetic contributions. Suppressing the dynamic relaxation channels with high fields ($B_0 \geq 10$ T), in principle, recovers the intrinsic electronic response, providing a promising route to answer the question about a spin gap in the triangular systems. Given the lack of a non-zero fermionic contribution to the low-temperature specific heat [40], the case for a gapped ground state is stronger for κ -HgCl than it is for κ -CuCN and κ -AgCN.

We thank N. Drichko, K. Kanoda, R. Valentí, S. Winter, M. Dressel and A.-M. Tremblay for useful comments and discussions. A. P. acknowledges support by the Alexander von Humboldt Foundation through the Feodor Lynen Fellowship. This work was supported by the National Science Foundation (DMR-1709304). Work performed in Frankfurt was supported by the Deutsche Forschungsgemeinschaft through the Transregional Collaborative Research Center SFB/TR49.

-
- [1] L. Balents, *Nature* **464**, 199 (2010).
- [2] L. Savary and L. Balents, *Rep. Prog. Phys.* **80**, 016502 (2017).
- [3] Y. Zhou, K. Kanoda, and T.-K. Ng, *Rev. Mod. Phys.* **89**, 25003 (2017).
- [4] P. W. Anderson, *Mater. Res. Bull.* **8**, 153 (1973).
- [5] H. Kino and H. Fukuyama, *J. Phys. Soc. Jpn.* **65**, 2158 (1996).
- [6] R. Kato, *Chem. Rev.* **104**, 5319 (2004).
- [7] Y. Shimizu, K. Miyagawa, K. Kanoda, M. Maesato, and G. Saito, *Phys. Rev. Lett.* **91**, 107001 (2003).
- [8] T. Itou, A. Oyamada, S. Maegawa, M. Tamura, and R. Kato, *Phys. Rev. B* **77**, 104413 (2008).
- [9] S. Yamashita, Y. Nakazawa, M. Oguni, Y. Oshima, H. Nojiri, Y. Shimizu, K. Miyagawa, and K. Kanoda, *Nat. Phys.* **4**, 459 (2008).
- [10] S. Yamashita, T. Yamamoto, Y. Nakazawa, M. Tamura, and R. Kato, *Nat. Commun.* **2**, 275 (2011).
- [11] D. Watanabe, M. Yamashita, S. Tonegawa, Y. Oshima, H. M. Yamamoto, R. Kato, I. Sheikin, K. Behnia, T. Terashima, S. Uji, T. Shibauchi, and Y. Matsuda, *Nat. Commun.* **3**, 1090 (2012).
- [12] Y. Shimizu, T. Hiramatsu, M. Maesato, A. Otsuka, H. Yamochi, A. Ono, M. Itoh, M. Yoshida, M. Takigawa, Y. Yoshida, and G. Saito, *Phys. Rev. Lett.* **117**, 107203 (2016).
- [13] M. Yamashita, N. Nakata, Y. Senshu, M. Nagata, H. M. Yamamoto, R. Kato, T. Shibauchi, and Y. Matsuda, *Science* **328**, 1246 LP (2010).
- [14] M. Dressel and A. Pustogow, *J. Phys. Condens. Matter* **30**, 203001 (2018).
- [15] A. Pustogow, Y. Saito, E. Zhukova, B. Gorshunov, R. Kato, T.-H. Lee, S. Fratini, V. Dobrosavljević, and M. Dressel, *Phys. Rev. Lett.* **121**, 056402 (2018).
- [16] The results from Ref. [13] have been recently challenged in Ref. [54].
- [17] A. Pustogow, M. Bories, A. Löhle, R. Rösslhuber, E. Zhukova, B. Gorshunov, S. Tomić, J. A. Schlueter, R. Hübner, T. Hiramatsu, Y. Yoshida, G. Saito, R. Kato, T.-H. Lee, V. Dobrosavljević, S. Fratini, and M. Dressel, *Nat. Mater.* **17**, 773 (2018).
- [18] K. Miyagawa, A. Kawamoto, Y. Nakazawa, and K. Kanoda, *Phys. Rev. Lett.* **75**, 1174 (1995).
- [19] Y. Shimizu, K. Miyagawa, K. Kanoda, M. Maesato, and G. Saito, *Phys. Rev. B* **73**, 140407 (2006).
- [20] H. C. Kandpal, I. Opahle, Y.-Z. Zhang, H. O. Jeschke, and R. Valentí, *Phys. Rev. Lett.* **103**, 67004 (2009); K. Nakamura, Y. Yoshimoto, T. Kosugi, R. Arita, and M. Imada, *J. Phys. Soc. Jpn.* **78**, 83710 (2009).
- [21] P. Lunkenheimer, J. Müller, S. Krohns, F. Schrettle, A. Loidl, B. Hartmann, R. Rommel, M. de Souza, C. Hotta, J. A. Schlueter, and M. Lang, *Nat. Mater.* **11**, 755 (2012).
- [22] M. Matsuura, T. Sasaki, S. Iguchi, E. Gati, J. Müller, O. Stockert, A. Piovano, M. Böhm, J. T. Park, S. Biswas, S. M. Winter, R. Valentí, A. Nakao, and M. Lang, *Phys. Rev. Lett.* **123**, 27601 (2019).
- [23] D. Guterding, R. Valentí, and H. O. Jeschke, *Phys. Rev. B* **92**, 81109 (2015).
- [24] D. A. Huse and V. Elser, *Phys. Rev. Lett.* **60**, 2531 (1988).
- [25] T. Furukawa, K. Miyagawa, T. Itou, M. Ito, H. Taniguchi, M. Saito, S. Iguchi, T. Sasaki, and K. Kanoda, *Phys. Rev. Lett.* **115**, 77001 (2015).
- [26] M. Dressel, P. Lazić, A. Pustogow, E. Zhukova, B. Gorshunov, J. A. Schlueter, O. Milat, B. Gumhalter, and S. Tomić, *Phys. Rev. B* **93**, 81201 (2016).
- [27] M. Pinterić, D. Rivas Góngora, Ž. Rapljenović, T. Ivek, M. Čulo, B. Korin-Hamzić, O. Milat, B. Gumhalter, P. Lazić, M. Sanz Alonso, W. Li, A. Pustogow, G. Gorgen Lesseux, M. Dressel, and S. Tomić, *Crystals* **8**, 190 (2018).
- [28] T. Itou, E. Watanabe, S. Maegawa, A. Tajima, N. Tajima, K. Kubo, R. Kato, and K. Kanoda, *Sci. Adv.* **3**, e1601594 (2017).
- [29] P. Lazić, M. Pinterić, D. Rivas Góngora, A. Pustogow, K. Treptow, T. Ivek, O. Milat, B. Gumhalter, N. Došlić, M. Dressel, and S. Tomić, *Phys. Rev. B* **97**, 245134 (2018).
- [30] K. Riedl, R. Valentí, and S. M. Winter, *Nat. Commun.* **10**, 2561 (2019).
- [31] B. J. Powell, E. P. Kenny, and J. Merino, *Phys. Rev. Lett.* **119**, 87204 (2017).
- [32] O. I. Motrunich, *Phys. Rev. B* **72**, 45105 (2005).
- [33] S. Yasin, E. Rose, M. Dumm, N. Drichko, M. Dressel, J. A. Schlueter, E. I. Zhilyaeva, S. Torunova, and R. N. Lyubovskaya, *Physica B: Condens. Matter* **407**, 1689 (2012).
- [34] N. Drichko, R. Beyer, E. Rose, M. Dressel, J. A. Schlueter, S. A. Turunova, E. I. Zhilyaeva, and R. N. Lyubovskaya, *Phys. Rev. B* **89**, 75133 (2014).
- [35] A. Löhle, E. Rose, S. Singh, R. Beyer, E. Tafra, I. R. E. I. Zhilyaeva, R. N. Lyubovskaya, and M. Dressel, *J. Phys. Condens. Matter* **29**, 55601 (2017).
- [36] T. Ivek, R. Beyer, S. Badalov, M. Čulo, S. Tomić,

- J. A. Schlueter, E. I. Zhilyaeva, R. N. Lyubovskaya, and M. Dressel, *Phys. Rev. B* **96**, 85116 (2017).
- [37] E. Gati, J. K. H. Fischer, P. Lunkenheimer, D. Zielke, S. Köhler, F. Kolb, H.-A. K. von Nidda, S. M. Winter, H. Schubert, J. A. Schlueter, H. O. Jeschke, R. Valentí, and M. Lang, *Phys. Rev. Lett.* **120**, 247601 (2018).
- [38] M. Hemmida, H.-A. K. von Nidda, B. Miksch, L. L. Samoilenko, A. Pustogow, S. Widmann, A. Henderson, T. Siegrist, J. A. Schlueter, A. Loidl, and M. Dressel, *Phys. Rev. B* **98**, 241202(R) (2018).
- [39] E. Gati, S. M. Winter, J. A. Schlueter, H. Schubert, J. Müller, and M. Lang, *Phys. Rev. B* **97**, 75115 (2018).
- [40] N. Hassan, S. Cunningham, M. Mourigal, E. I. Zhilyaeva, S. A. Torunova, R. N. Lyubovskaya, J. A. Schlueter, and N. Drichko, *Science* **360**, 1101 LP (2018).
- [41] N. M. Hassan, K. Thirunavukkuarasu, Z. Lu, D. Smirnov, E. Zhilyaeva, S. Torunova, R. Lyubovskaya, and N. Drichko, (2019), arXiv:1905.12740.
- [42] While for κ -(BEDT-TTF)₂Hg(SCN)₂Cl $t_a/t' \approx 3$, the paradigmatic κ -phase materials κ -CuCN, κ -AgCN and κ -CuCl have larger ratios of approximately 4–5.
- [43] Y. Yue, K. Yamamoto, M. Uruichi, C. Nakano, K. Yakushi, S. Yamada, T. Hiejima, and A. Kawamoto, *Phys. Rev. B* **82**, 75134 (2010).
- [44] T. Ivek, B. Korin-Hamzić, O. Milat, S. Tomić, C. Clauss, N. Drichko, D. Schweitzer, and M. Dressel, *Phys. Rev. B* **83**, 165128 (2011).
- [45] The spectrum is actually comprised of a superposition of 8 inequivalent but unresolved protons sites. See Supplemental Material for angle-dependent measurements.
- [46] D. C. Johnston, *Phys. Rev. B* **74**, 184430 (2006).
- [47] T. Itou, A. Oyamada, S. Maegawa, and R. Kato, *Nat. Phys.* **6**, 673 (2010).
- [48] M. Poirier, S. Parent, A. Côté, K. Miyagawa, K. Kanoda, and Y. Shimizu, *Phys. Rev. B* **85**, 134444 (2012).
- [49] Upon proper renormalization to the gyromagnetic ratios and the local charge density, cf. Fig. 4(a) in Ref. 12, the ¹H and ¹³C data coincide in the relevant temperature range ($k_B T \leq J$) when acquired at the same magnetic field. Upon changing B_0 , the apparently intrinsic response at temperatures above the maximum remains unaltered, while the low- T behavior exhibits pronounced modifications, including suppression by field [12].
- [50] F. L. Pratt, P. J. Baker, S. J. Blundell, T. Lancaster, S. Ohira-Kawamura, C. Baines, Y. Shimizu, K. Kanoda, I. Watanabe, and G. Saito, *Nature* **471**, 612 (2011).
- [51] T. Isono, T. Terashima, K. Miyagawa, K. Kanoda, and S. Uji, *Nat. Commun.* **7**, 13494 (2016); T. Isono, S. Sugiura, T. Terashima, K. Miyagawa, K. Kanoda, and S. Uji, *ibid.* **9**, 1509 (2018).
- [52] R. Świetlik, B. Barszcz, A. Pustogow, and M. Dressel, *Phys. Rev. B* **95**, 85205 (2017).
- [53] K. G. Padmalekha, M. Blankenhorn, T. Ivek, L. Bogani, J. A. Schlueter, and M. Dressel, *Physica B: Condens. Matter* **460**, 211 (2015).
- [54] P. Bourgeois-Hope, F. Laliberté, E. Lefrançois, G. Grissonanche, S. René de Cotret, R. Gordon, S. Kitou, H. Sawa, H. Cui, R. Kato, L. Taillefer, and N. Doiron-Leyraud, (2019), arXiv:1904.10402.

SUPPLEMENTAL MATERIAL

Impurity Density Estimate

The impurity spin density, N , of κ -(BEDT-TTF)₂Hg(SCN)₂Cl was estimated by analyzing the Curie-like region of the spin susceptibility below 15 K. In order to assign absolute values to the ESR data from Ref. [S1] (Fig. S7 in Supplementary Materials), we scaled the ESR intensity to match typical values of κ -compounds in the range above the maximum, i.e. $10 \text{ K} \leq T \leq 30 \text{ K}$. In Fig. S1 we plot χ_{ESR} and scale it to match with the susceptibility of κ -(BEDT-TTF)₂Cu₂(CN)₃ [S2], which has similar structural properties and exchange energy. The Curie-Weiss fit below 15 K yields a molar Curie constant $C_{mol} \approx 0.006 \text{ emuK/mol}$. From the Curie law

$$C = \frac{\mu_0 \mu_B^2}{3k_B} N g^2 (S(S+1)) = \chi T \quad (\text{S1})$$

we obtain the relation

$$N = \frac{k_B C_{mol}}{\mu_0 \mu_B^2 N_A} \quad (\text{S2})$$

where N is the number of impurities per unit cell and we used the values $S = 1/2$, $g = 2$ and $V_{UC} = 3500 \text{ \AA}^3$ [S3]. Plugging in the above determined value of C_{mol} , we obtain $N = 0.016 \text{ spins/unit cell}$. This impurity spin density corresponds to an average distance between protons and impurities on the order of a few nm.

Since for paramagnets $\chi T \propto T_1^{-1}$, it is reasonable to use Fig. 4(c,d) to extrapolate the impurity spin densities for κ -(BEDT-TTF)₂Cu₂(CN)₃ and κ -(BEDT-TTF)₂Ag₂(CN)₃ from their T_1^{-1} , using the same C . The results of this calculation are shown in Table S1.

As an independent check, we now estimate the average distance between ¹H nuclear spins in κ -HgCl and the impurity spins based on Eq. (1). For that, we approximated τ from the ESR linewidth in the insulating state [S1]. For $\Delta H = 30 \text{ G}$, uncertainty principle yields a mutual spin flip rate of $\Delta t = \tau = 9.5 * 10^{-10} \text{ s}$. Solving Eq. (1) [S7] in the low-frequency limit, using $T_1 = 10 \text{ s}$, we obtained $r = 7 \text{ nm}$, which is comparable to the approximation above obtained from the impurity density N via the Curie constant C . *Vice versa*, this means that there is even quantitative

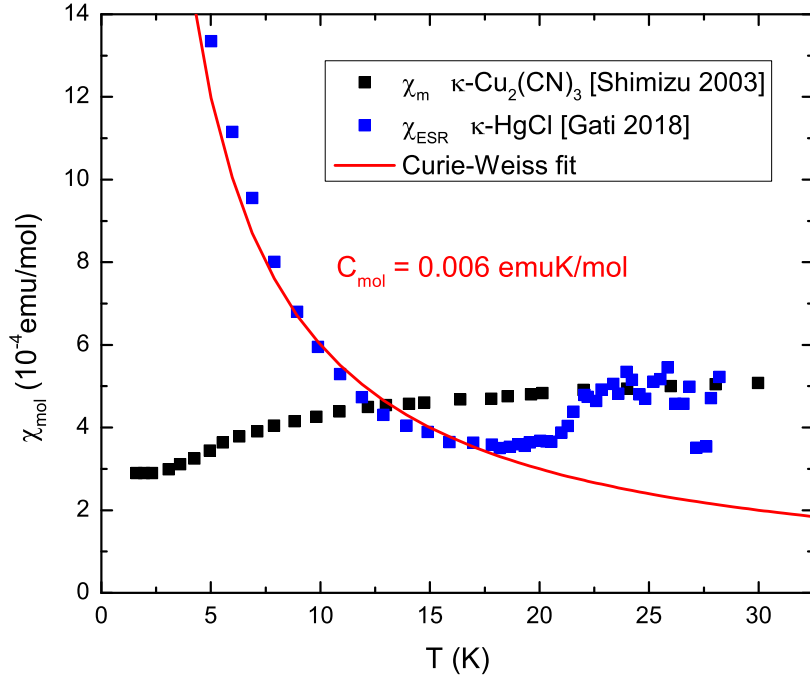


FIG. S1. The absolute values of the spin susceptibility of κ -(BEDT-TTF)₂Hg(SCN)₂Cl (determined by ESR measurements in Ref. [S1]) was approximated by χ_{mol} of κ -(BEDT-TTF)₂Cu₂(CN)₃ [S2].

Compound	$1/T_1$ (1/s)	C (emuK/mol)	V_{UC} (\AA^3)	N
κ -Hg-Cl	0.1	0.006	3500 [S3]	0.016
κ -Ag-CN	0.04	0.0024	1756 [S4]	0.0064
κ -Cu-CN	0.03	0.0018	1695 [S5]	0.0048

TABLE S1. Relaxation rate at the maximum, Curie constant, unit cell volume and resulting impurity spin density N (per unit cell) for κ -(BEDT-TTF) $_2$ Hg(SCN) $_2$ Cl, κ -(BEDT-TTF) $_2$ Cu $_2$ (CN) $_3$ [S5], and κ -(BEDT-TTF) $_2$ Ag $_2$ (CN) $_3$ [S4, S6].

agreement (within a factor two, given the approximations made) of the experimentally observed T_1 with the discussed model of dipolar coupling between protons and impurity spins.

NMR Spectra Upon Rotation

In order to evaluate the ^1H NMR spectra, we performed angle-dependent measurements at 1.8 K using a piezoelectric rotator. While the line shape in Fig. 2 of the main manuscript shows a trident-like structure, Fig. S2 reveals four main peaks that follow a common angle dependence. At the angle where temperature-dependent experiments were carried out (0°) the two inner peaks are simply too close together to be distinguished. Given this proximity of the peaks, and generally reduced signal-noise ratio at elevated temperatures, we did not observe any changes in the spectrum upon crossing the glass transition at $T_g = 63$ K (cooling rate 0.5 K/min). As the focus of the present study was on low temperatures, the limited number of T_1 data points around T_g does not capture the glass transition. Future work could target on this interesting variant, where only one (of the two) ethylene endgroups is involved [S8], which constitutes a potential source of disorder in the system, e.g. dependent on the cooling rate through T_g .

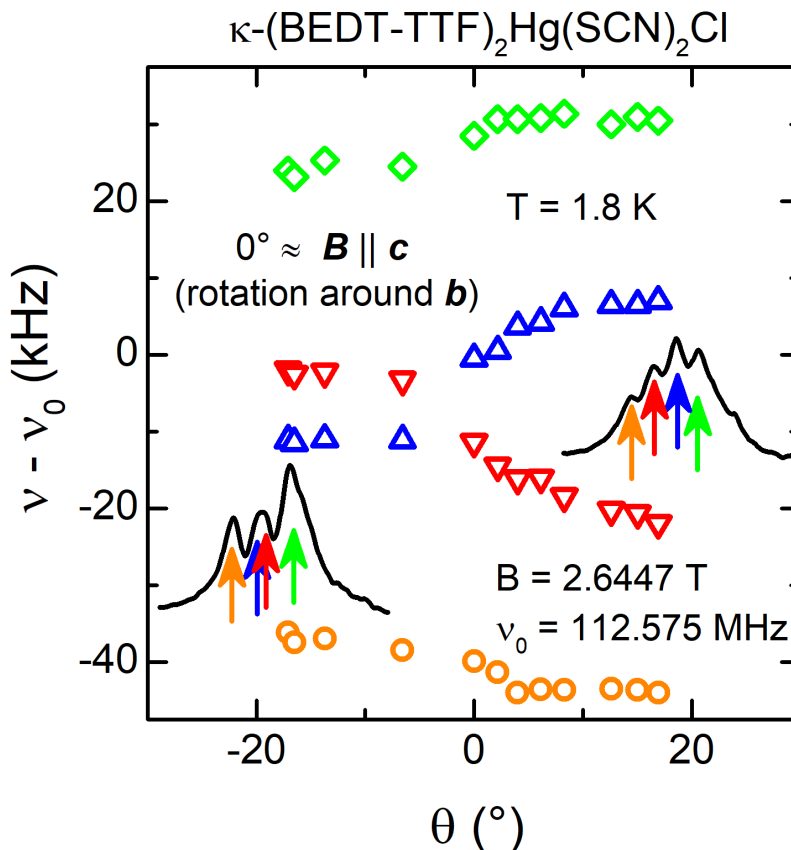


FIG. S2. NMR spectra upon rotation reveal four main modes. The temperature-dependent measurements presented in the main manuscript were performed at $\theta = 0^\circ$, which is close to the crystallographic c -axis.

-
- [S1] E. Gati, J. K. H. Fischer, P. Lunkenheimer, D. Zielke, S. Köhler, F. Kolb, H.-A. K. von Nidda, S. M. Winter, H. Schubert, J. A. Schlueter, H. O. Jeschke, R. Valentí, and M. Lang, *Phys. Rev. Lett.* **120**, 247601 (2018).
- [S2] Y. Shimizu, K. Miyagawa, K. Kanoda, M. Maesato, and G. Saito, *Phys. Rev. Lett.* **91**, 107001 (2003).
- [S3] N. Drichko, R. Beyer, E. Rose, M. Dressel, J. A. Schlueter, S. A. Turunova, E. I. Zhilyaeva, and R. N. Lyubovskaya, *Phys. Rev. B* **89**, 75133 (2014).
- [S4] Y. Shimizu, T. Hiramatsu, M. Maesato, A. Otsuka, H. Yamochi, A. Ono, M. Itoh, M. Yoshida, M. Takigawa, Y. Yoshida, and G. Saito, *Phys. Rev. Lett.* **117**, 107203 (2016).
- [S5] H. O. Jeschke, M. de Souza, R. Valentí, R. S. Manna, M. Lang, and J. A. Schlueter, *Phys. Rev. B* **85**, 35125 (2012).
- [S6] T. Hiramatsu, Y. Yoshida, G. Saito, A. Otsuka, H. Yamochi, M. Maesato, Y. Shimizu, H. Ito, Y. Nakamura, H. Kishida, M. Watanabe, and R. Kumai, *Bull. Chem. Soc. Jpn.* **90**, 1073 (2017).
- [S7] A. Abragam, *Principles of Nuclear Magnetism* (Oxford University Press, Hong Kong, 1983).
- [S8] E. Gati, S. M. Winter, J. A. Schlueter, H. Schubert, J. Müller, and M. Lang, *Phys. Rev. B* **97**, 75115 (2018).